Journal of the Serbian Society for Computational Mechanics / Vol. 18 / No. 2, 2024 / pp 96-109 / original paper
(10.24874/jsscm.2024.18.02.06)

INVERSE IDENTIFICATION METHOD OF PLASTICITY PARAMETERS OF ANISOTROPIC MATERIAL

Dao Lien Tien[1] [0009-0004-5099-3714] and Viet Dung Luong[1*] [0000-0002-3093-837X]

[1] Faculty of Mechanical Engineering, Thai Nguyen University of Technology, Vietnam
e-mail: daotien@tnut.edu.vn, luongvietdung@tnut.edu.vn
*c*orresponding author*

Abstract

Nowadays, the finite element method has been widely applied in product calculation and design. One of the critical parameters in finite element modeling are the parameters in the material behavior model. In this study, an inverse procedure determines the values of parameters in the behavior model of anisotropic materials. First, optimization algorithms are used to evaluate the deviation between experimental data and numerical simulations. Based on that, the corresponding parameter values need to be determined. The accuracy of the parameter values determined by the proposed method is evaluated by comparing the numerical simulation results with the experimental results. This process can also be applied to many different mechanical behaviors of materials.

Keywords: parameter identification, optimization algorithm plastic, finite element, simulation, corrugated.

1. Introduction

Material parameters are very important in finite element modeling (FEM). The accuracy of these parameters, such as elastic modulus, tensile strength, Poisson's ratio, work hardening properties, and several other coefficients, can significantly affect the numerical simulation results of the model. Many methods have been used to accurately determine these parameters, such as inverse methods, optimization algorithms, and experimental calibration. However, each study used a different approach, even though the same technique was used. Cooreman et al. (2007) developed an inverse method for determining material parameters in elastic-plastic materials. The study focused on studying the influence of the sensitivity matrix to changes in material parameters on the mechanical behavior of the material. Digital image correlation (DIC) was used to determine the exact parameters in real-time to improve the accuracy of material models when provided with experimental data. Inverse techniques were then used to estimate material parameters by minimizing the difference between experimental observations and model predictions in S. Cooreman's study (Cooreman et al. 2008). A recent study that combined experimental data from DIC and an advanced optimization method (ensemble-based 4DVar) in Stefan Hartmann's study (Stefan Hartmann 2021) allows for a more accurate simulation of material behavior, especially usable with highly noisy data. In another study, a hybrid inverse analysis method is proposed by Zhang et al. (2010) to determine the nonlinear material parameters in the mechanical behavior of composite material. This method combines experimental and numerical methods with the inverse search method to determine the nonlinear material parameters of each component layer in a plate.

The number of material parameters to be determined depends on the material type used and the study's behavior model. One behavioral model that frequently appears in research is the Johnson-Cook model ((D. Remache et al. 2019), Wangtian Yin and Yongbao Liu (2024), Titu et al. (2021), Jiang et al. (2024), Aghdami and Davoodi (2020), Özel and Karpat (2007)). In these studies, the way of determining the parameters in the material model is not the same. The Levenberg-Marquardt optimization algorithm used in the study of Shrot and Bäker (2012) improved the accuracy in determining the parameters of 6063-T5 aluminum alloy in the Johnson-Cook behavior model. The Newton-Raphson method with the objective function determined based on the difference between the analytical and experimental tensile forces was used in the study of Ashkan Mahmoud Aghdami et al. (2020) to determine the values of the parameters in the Johnson-Cook behavioral model. In the study of Wang et al. (2023), the Johnson-Cook constitutive model was modified to more accurately predict the mechanical behavior of 6063-T5 aluminum alloy under high temperature and dynamic conditions. On that basis, the accuracy of material parameter values was improved.

In addition, in many other studies, determining material parameters in finite element models is also mentioned such as the studies of Abdullah, Kuntjoro, and Yamin (2017), Li et al. (2021), Dorogoy and Rittel (2009), Jebri et al. (2022), Hor et al. (2013), Murugesan and Jung (2019), and Laakso and Niemi (2016), Tien et al (2024), Tien et al (2023), Luong et al. (2023), and Mrówczyński et al (2022). However, most of these studies have not mentioned the use of multi-objective methods to increase the determinism of the problem. In addition, published studies also show that the material parameter determination procedures are mainly limited to isotropic materials, the steps in the inverse identification method are unclear, and the possibility of extending the procedure to other materials is not mentioned.

This study proposes an inverse method for determining the parameters of anisotropic materials. The accuracy of the obtained results is verified by comparing the experimental results and numerical simulations of carton compression tests. This process can be easily applied to various material behavior models.

2. Research material and mechanical behavior model

2.1. Material

Anisotropic materials exhibit different mechanical behavior in various directions. The material used in this study is corrugated cardboard. It consists of three layers of paper: Liner and fluting (Fig.1). The manufacturing process gives three characteristic directions: the machine direction (MD), the cross direction (CD), and the thickness direction (ZD). Characteristics of each layer in corrugated cardboard are shown in Table 1 and Fig.2.

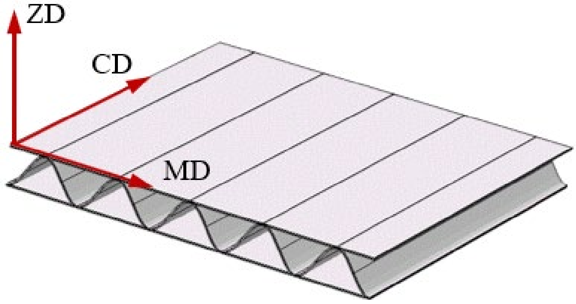

Fig. 1. Geometric structure and the directions of the corrugated cardboard panel

	Grammage (g/mm^2)	Thickness (mm)
Liner	140	0.18±0.004
Fluting	113	0.15±0.008

Table 1. Cardboard plate properties

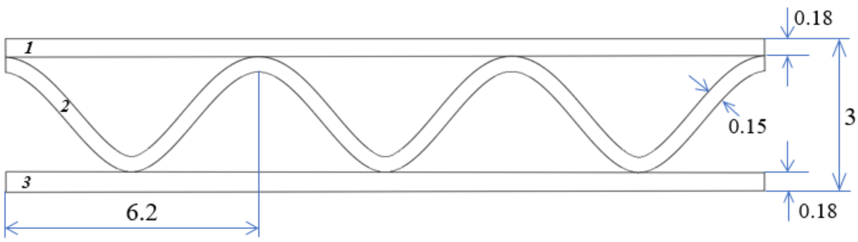

Fig. 2. Dimensional characteristics of corrugated cardboard plate (all dimensions are in mm)

2.2. Paper material behavior model

Due to the small thickness of the cardboard, the out-of-plane properties are difficult to determine. In the study of Stenberg (Niclas Stenberg 2003), it was shown that Young's modulus in the perpendicular direction (ZD) is about 200 times lower than that of MD. At the same time, the study of Stenberg et al. (N. Stenberg, Fellers, and Östlund 2001) also showed that the in-plane deformation during compression with thickness is negligible. Therefore, the Poisson's ratios γ_{xz} and ν_{yz} are close to zero.

Paper exhibits anisotropic properties. In this study, we use the Isotropic Plasticity Equivalent model (IPE) to describe the behavior of paper (Mäkelä and Östlund 2003). The orthotropic elasticity behavior in-plane stresses is defined by:

$$\{\sigma\} = \begin{Bmatrix} \sigma_x \\ \sigma_y \\ \sigma_{xy} \end{Bmatrix} = [H]\{\varepsilon^e\} = \frac{1}{(1-\nu_{xy}\nu_{yx})} \begin{pmatrix} E_x & \nu_{yx}E_x & 0 \\ \nu_{xy}E_y & E_y & 0 \\ 0 & 0 & G_{xy}(1-\nu_{xy}\nu_{yx}) \end{pmatrix} \begin{Bmatrix} \varepsilon_x{}^e \\ \varepsilon_y{}^e \\ \gamma_{xy}{}^e \end{Bmatrix} \tag{1}$$

The yield criterion was formulated by Mäkelä and Östlund (2003) as:

$$f = \sigma_{eq} - \sigma_y = \left(\frac{3}{2} < s > \{s\}\right)^{1/2} - E_0(\varepsilon_0 + \varepsilon_{eq}^p)^{1/n} \tag{2}$$

where σy is the plasticity threshold, ε_{eq}^p is the equivalent plastic strain, E0 and n are the stiffness modulus and stiffness exponent, respectively, $\{s\}$ is the deviatoric stress row vector defined in Eq. (3), and $\langle s\rangle$ is its transpose ($\langle s\rangle = \{s\}T$).

The deviatoric stresses vector and the IPE plasticity criterion are given by:

$$\{s\} = \begin{Bmatrix} s_x \\ s_y \\ s_z \\ s_{xy} \end{Bmatrix} = [L]\{\sigma\} = \frac{1}{3}\begin{pmatrix} 2a & c-a-b & 0 \\ c-a-b & 2b & 0 \\ b-c-a & a-b-c & 0 \\ 0 & 0 & 3d \end{pmatrix}\begin{Bmatrix} \sigma_x \\ \sigma_y \\ \sigma_{xy} \end{Bmatrix} \tag{3}$$

where L is a fourth-order invariant transformation tensor and it satisfies the symmetry conditions; a, b, c, d, and n describe the anisotropy of the material which can be identified from the experimental traction curves (see next section). This model will be implemented in the Abaqus/Explicit software using the VUMAT user subroutine.

3. Inverse method

The mechanical behavior of materials is expressed through the relationship between force vs displacement or stress vs strain obtained after performing tensile tests. Therefore, the graphs representing these relationships are often used to determine the values of parameters corresponding to each material behavior model. Based on the definition of “curve fitting” by Piegl (1988), inverse identification methods have been used to determine the system parameters that cannot be measured directly. In contrast, the values of these parameters directly affect the model output. Many techniques have been proposed to solve inverse problems.

For material behavior modeling, the quantitative values of parameters in the material model are difficult to determine directly from experiments. The proposed method is developed by iteratively minimizing the deviation between the experimentally measured quantities and the numerically calculated quantities. The objective function used is a least-squares scalar function consisting of the difference between the numerical calculation and the experimental measurement of the force-displacement curve as shown in expression (4):

$$F_{obj} = \frac{1}{N}\sum_{i=1}^{N}\left(F_{num}\left(U_{num}\right) - F_{\exp}\left(U_{\exp}\right)\right)^2 \tag{4}$$

Where N is the number of data sets, U_{num} and U_{exp} are the numerical and experimental displacement, and F_{num} and F_{exp} are the tensile forces determined by numerical simulation and measured experimentally, respectively. The flowchart of the identification process is shown in Fig. 3. The main steps in the process of determining the parameters of the IPE model for the materials used in this study:

3.1 Perform experiments

In this section, tensile tests on the research material will be conducted to determine the experimental data (force-displacement relationship data).

3.2 Finite element simulation of the tensile test

Perform numerical simulations of the experiments conducted in the previous section. From there, the data needed for the inverse determination process will be determined.

3.3 Select optimization algorithm

There are many optimization algorithms in use today. The genetic algorithm (GA), based on the principles of genetics and natural selection, allows a population of individuals to evolve according to specific selection rules to a state that minimizes the cost function by finding a local minimum. Therefore, several multi-objective evolutionary algorithms based on GA have been developed such as Multi-Objective Genetic Algorithm (MOGA), Pareto Niche Genetic Algorithm (NPGA), Weighted Genetic Algorithm (WBGA), Randomly Weighted Genetic Algorithm (RWGA), etc. Among them, MOGA-II is an improved version of MOGA, which was proposed by Poloni et al (Poloni et al. 2000). Research by Saha and Bandyopadhyay (2013) has shown that MOGA-II uses intelligent multi-objective search to achieve efficiency and directional intervention to achieve fast convergence. Compared with other algorithms, the advantages of MOGA-II are good stability, low sensitivity to termination at local extrema, and adaptability to nonlinear problems. MOGA-II requires very few user-supplied parameters, and some other parameters are interpolated to improve the efficiency of the optimization process. In particular, the convergence speed is fast. Therefore, the MOGA-II algorithm is used in this study.

In addition, the numerical optimization process is performed in the ModeFRONTIER 4.0 software. ModeFRONTIER is a multi-objective design and optimization environment, written to easily combine CAD/CAE tools and finite element structural analysis. Many standard or advanced optimization algorithms exist. They can be used depending on the complexity of the problem to be solved. The general procedure for inverse determination of parameters in modeFrontier is shown in Figure 4.

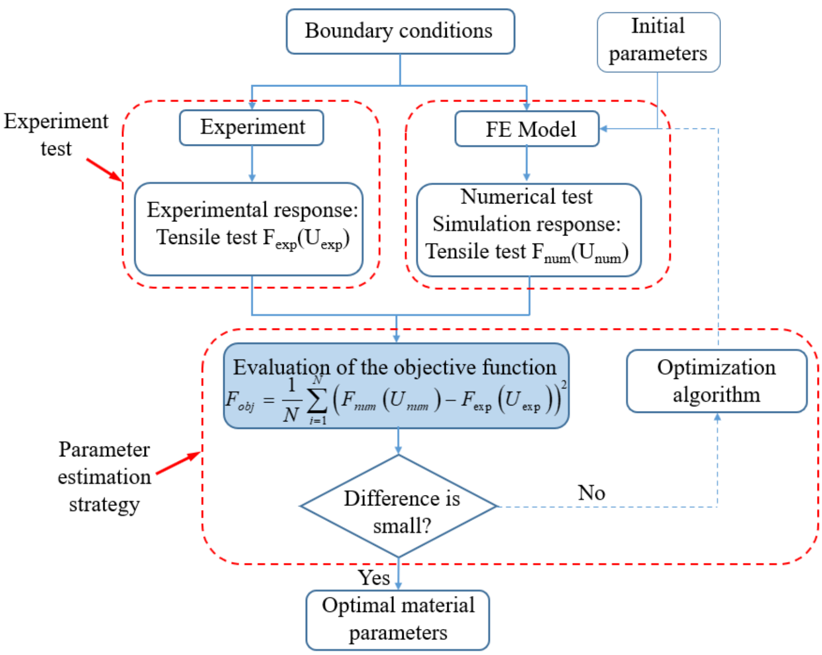

Fig. 3. Identification method by the inverse method

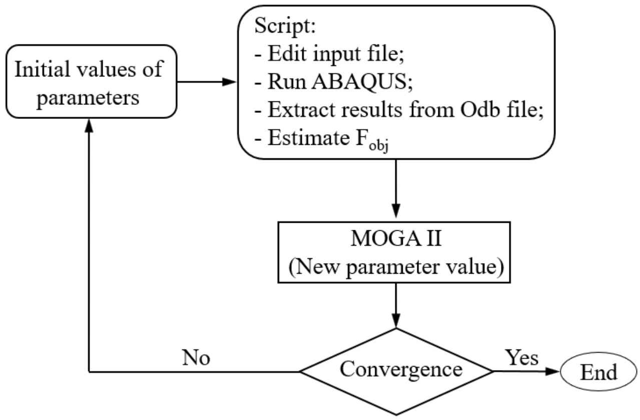

Fig. 4. General procedure for determining parameters

3.4 The optimization process to determine the IPE model parameters

Main tasks in this step:

- Select and extract test data of the force-displacement curve;
- Simulate tensile test in three directions using ABAQUS software;
- Extract force and displacement values from the ODB file (Abaqus) using Python script;
- Evaluate the objective function given in equation (4);
- Update the set of constitutive parameters using the MOGA-II genetic algorithm;
- Determine the set of material parameters for the optimal solution.

4. Results and discussion

The proposed inverse determination procedure is used to determine the parameters in the IPE model for paper material. The determined parameters will be fed into a numerical simulation model of a compressed carton box. The obtained results will be compared with experimental results to evaluate the reliability of the proposed identification procedure.

4.1. Experiment

To separate the paper layers from the corrugated core cardboard, the cardboard sheets are soaked in water to allow the paper layers to peel off. The flat sheets are then kept at 23°C and 50% relative humidity (RH) for several days to allow the paper to dry. The specimens used for tensile testing are designed with the shape and size shown in Figure 5. The paper specimens are cut in three directions: MD, CD, and 45° for each paper layer (Fig.6 and Fig.7). To ensure the clamping jaws grip more firmly when placing the specimen, cardboard pieces are glued to the two sides of the two ends of the tensile specimen. The tensile test results of paper specimens are presented as force-displacement curves as shown in Figs. 8 and 9.

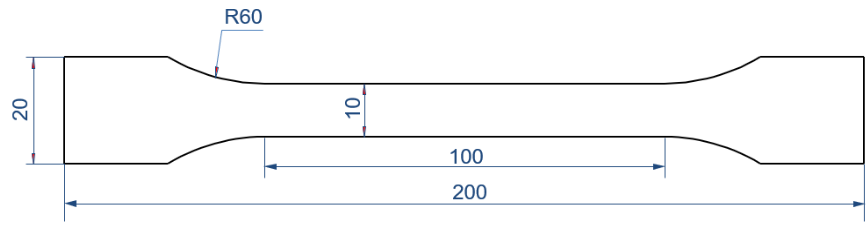

Fig. 5. The dimensions of the tensile test specimen

Fig. 6. Tensile specimens of papers 1 and 3

Fig .7. Tensile specimens of paper 2

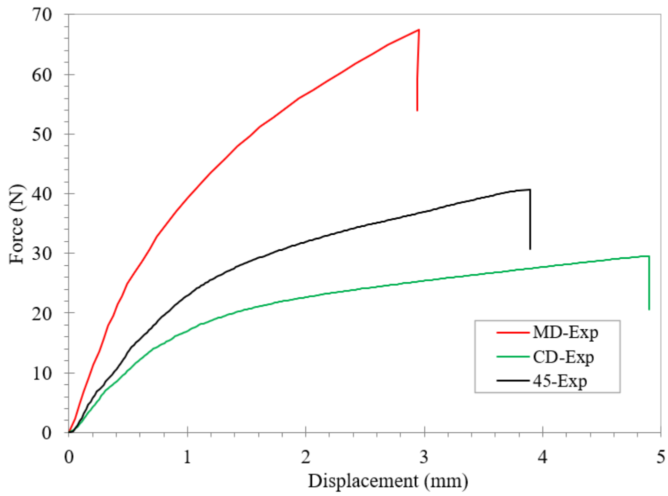

Fig. 8. Force vs displacement relationship of paper specimens 1 and 3

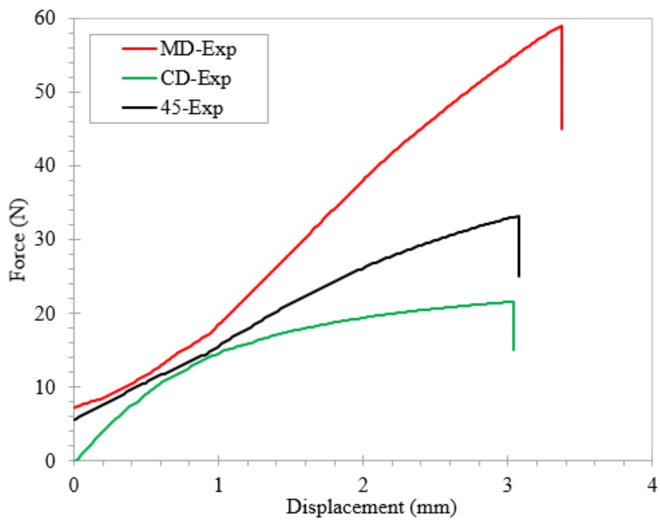

Fig. 9. Force vs displacement relationship of paper specimen 2

4.2. Finite element simulation of the tensile test

Finite element simulations of the tensile tests of paper specimens were performed using Abaqus software. The FEM model size of the simulated specimen was taken the same as the tensile specimen size in the tensile test in the previous section. The selection of the element size in the FEM model should be based on the balance between the computation time and the accuracy of the model. Therefore, the specimen was discretized using 1038 four-node linear quadrilateral elements (S4R), and the element size was 1mm (Fig. 10). Furthermore, based on the experimental conditions, all simulations were performed under the same conditions as the tensile test. In addition, the FEM model of the simulated specimen considered material nonlinearity and geometric nonlinearity. Numerical simulations were performed on a computer with Intel Xeon Dell Precision T7810 E5-2667 v3 CPU (3.20 GHz), 32 GB RAM.

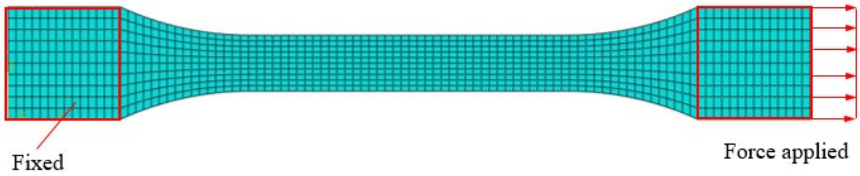

Fig. 10. Mesh and boundary conditions of tensile specimen

4.3. The optimization process

During the optimization process, the boundaries of eleven design variables are provided in Tables 2 and 3. A number of the initial design of experiments (DOE) was set to 12 designs by the Sobol algorithm, and the number of generations was set to 200.

Design variables	E_x (MPa)	E_y (MPa)	ν_{xy}	G_{xy} (MPa)	E_0
Lower bound	2000	500	0.05	500	50
Upper bound	3000	1500	0.4	1500	650

Table 2. Boundaries of design variables (elastic properties) in IPE's model

Design variables	n	A	B	C	D	ε_0
Lower bound	1.5	1	1	1	1	0.001
Upper bound	5	1	3	3	3	0.02

Table 3. Boundaries of design variables (plastic properties) in IPE's model

At the end of the reverse identification process, the results are shown in Figs. 11 and 12. Figure 11 shows that the parameter values of the IPE model accurately describe the paper behavior and a good agreement is observed between the experimental force-displacement curve and the finite element prediction. In Figure 12, there is a difference between the simulation results and the experimental results. This is the graph of the corrugated core layer when pressed flat to create tensile test samples in MD, CD, and 45^0 directions, causing the material's mechanical properties to change at the bending position of the paper. This leads to differences between simulation and experimental results, especially in the MD direction. On the other hand, in the corrugated board structure, the corrugated core does not undergo tension in the MD direction. Therefore, the error for the core board is acceptable. The parameter values obtained are shown in Tables 4 and 5, respectively. To check the accuracy of the determined material parameter values, a carton compression test was conducted. The box has dimensions as shown in Figure 13. Compression tests were performed on an INSTRON 4204 machine with a load of 5 kN (Fig.14). At the same time, a numerical simulation of carton compression test was also conducted. The finite element model uses the material parameters in Tables 4 and 5. Note that the plastic behavior model of paper is not available in finite element analysis software. Therefore, it is necessary to build a subroutine VUMAT to implement the IPE model in Abaqus software as in the studies of Tien et al (2024), Tien et al (2023), and Luong et al. (2023) comparing the experimental results and numerical simulations obtained in Figure 15. Note that when performing the carton compression test, the carton panels are compressed and folded. When the boxes are compressed, the cardboard sheets are compressed and folded differently in each test. This leads to the curves not matching between compression tests. However, this deviation is within acceptable limits.

Figure 15 shows that there is good agreement between the experimental curve and the numerical simulation. This proves that the material parameter values in the IPE model determined by the proposed method are accurate and reliable.

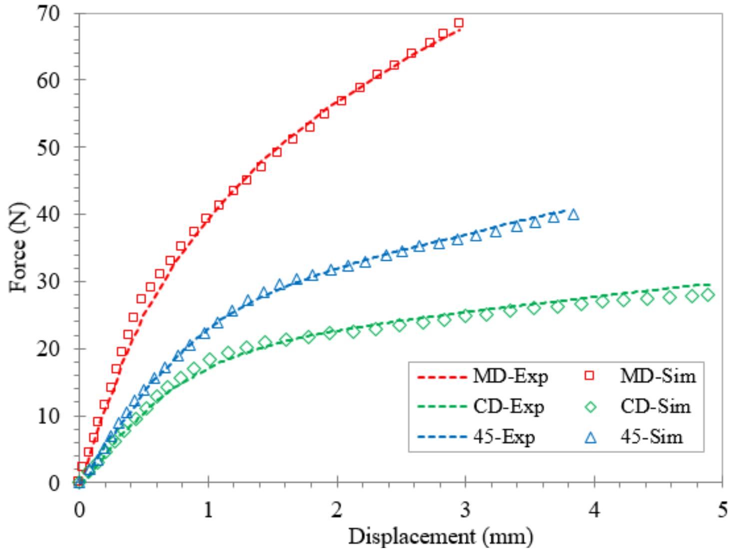

Fig. 11. Experimental and numerical simulation curves of papers 1 and 3

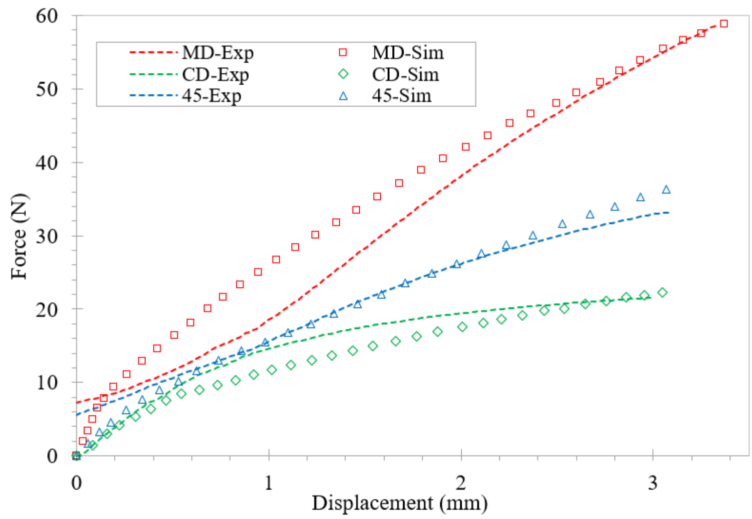

Fig. 12. Experimental curve and numerical simulation of paper 2

Paper layer	E_x (MPa)	E_y (MPa)	ν_{xy}	G_{xy} (MPa)	E_0
1,3	2350.2	879.91	0.0829	1047.2	91.45
2	1120.4	615.85	0.0717	301.05	80.31

Table 4. Elastic properties of the paper

Paper layer	n	A	B	C	D	ε_0
1,3	3.807	1.0	2.136	2.136	1.422	0.48e-3
2	3.047	1.0	2.718	2.136	1.571	0.92e-3

Table 5. Plastic properties of the paper

Fig.13. Dimensions of the compression box (all dimensions are in mm)

Fig.14. Experiment setup on INSTRON 4204 compression testing machine

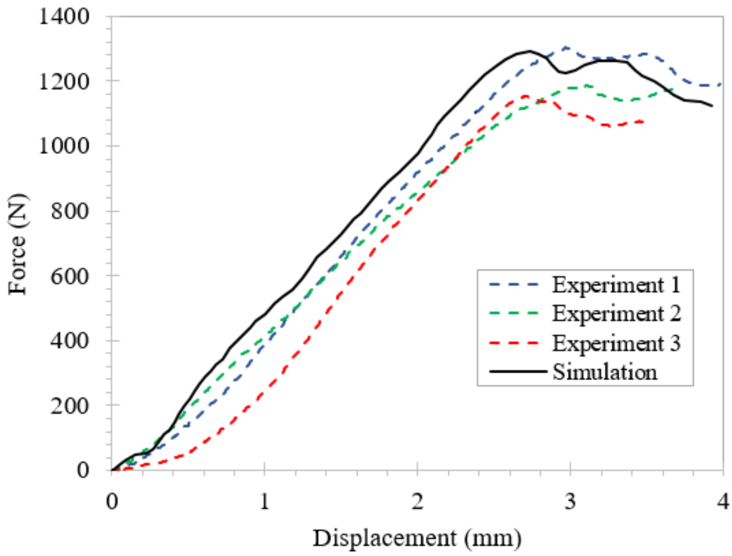

Fig.15. Comparison between experimental and numerical compression curves of carton box

5. Conclusions

This study proposed and developed an inverse procedure to determine the parameters in the paper material behavior model. This helps to improve the accuracy of numerical simulation of the material mechanical properties. The proposed procedure, which combines analysis and evaluation of experimental data and numerical simulation, has determined the important parameters in the plastic behavior model of paper materials. The parameters in the IPE model of the paper that have been determined are applied to simulate the compression carton box. A comparison of the obtained numerical curve with the experimental curve shows a good agreement. The research results show that the proposed procedure can determine accurate and reliable parameter values, thereby helping to optimize the simulation model. This procedure can be applied to other anisotropic and isotropic materials by modifying the material behavior model during the numerical simulation step of the inverse determination process. This study makes an important contribution to the design of packaging and industrial paper products. However, there are still some limitations such as not considering the impact of environmental factors such as humidity and temperature on the accuracy of the model. The results of this study provide a solid basis for further research to address remaining issues.

Acknowledgments: This research is supported by the Thai Nguyen University of Technology.

References:

Abdullah, AS, Kuntjoro W and Yamin AFM (2017). Finite Element Modelling of Aluminum Alloy 2024-T3 under Transverse Impact Loading, AIP Conference Proceedings 1901, 050005

Aghdami, AM, and Davoodi B (2020). An Inverse Analysis to Identify the Johnson-Cook Constitutive Model Parameters for Cold Wire Drawing Process, Mechanics and Industry 21 (5).

Cooreman S, Lecompte D, Sol H, Vantomme J, and Debruyne D (2007). Elasto-Plastic Material Parameter Identification by Inverse Methods: Calculation of the Sensitivity Matrix, International Journal of Solids and Structures 44 (13): 4329–41.

Dorogoy A, and Rittel D (2009). Determination of the Johnson-Cook Material Parameters Using the SCS Specimen, Experimental Mechanics 49 (6): 881–85.

Hor A, Morel F, Lebrun JL, and Germain G (2013). Modelling, Identification and Application of Phenomenological Constitutive Laws over a Large Strain Rate and Temperature Range, Mechanics of Materials 64: 91–110.

Jebri L, Lazghab T, Toumi M, and Soula M (2022). The Behavior and Forming Performance of Vapor Hydroforming Process of Thin Aluminum Sheets: Numerical and Experimental Analysis, Advances in Mechanical Engineering 14 (4).

Jiang, Xinyang, Jinfu Ding, Chengwu Wang, E. Shiju, Ling Hong, Weifeng Yao, Huadong Wang, Chongqiu Zhou, and Wei Yu. (2024). Parameter Identification of Johnson–Cook Constitutive Model Based on Genetic Algorithm and Simulation Analysis for 304 Stainless Steel, Scientific Reports 14 (1).

Laakso, Sampsa Vili Antero, and Esko Niemi. (2016). Modified Johnson-Cook Flow Stress Model with Thermal Softening Damping for Finite Element Modeling of Cutting, Proceedings of the Institution of Mechanical Engineers, Part B: Journal of Engineering Manufacture 230 (2): 241–53.

Li, Suyang, Jianbo Sui, Feng Ding, Shixiong Wu, Wanglin Chen, and Chengyong Wang. (2021). Optimization of Milling Aluminum Alloy 6061-T6 Using Modified Johnson-Cook Model, Simulation Modelling Practice and Theory 111.

Lien Tien Dao, Pham Tuong Minh Duong, Viet Dung Luong. (2024). Analysis of Stress and Strain in Sandwich Structures Using an Equivalent Finite Element Model, International Journal of Engineering and Technology Innovation. https://doi.org/https://doi.org/10.46604/ijeti.2024.

Luong, Viet Dung, Pham Tuong Minh Duong, Thi Bich Ngoc Nguyen, Nhu Khoa Ngo, Thi Hoa Nguyen, and Van Du Nguyen. (2023). Dynamic Response of High-Power Ultrasonic System Based on Finite Element Modeling of Piezoelectric, Journal of Applied Engineering Science 21 (3): 859–71.

Mäkelä, Petri, and Sören Östlund. (2003). Orthotropic Elastic-Plastic Material Model for Paper Materials, International Journal of Solids and Structures 40 (21): 5599–5620.

Mrówczyński, Damian, Anna Knitter-Piątkowska, and Tomasz Garbowski. (2022). Numerical Homogenization of Single-Walled Corrugated Board with Imperfections, Applied Sciences (Switzerland) 12 (19).

Murugesan, Mohanraj, and Dong Won Jung. (2019). Johnson Cook Material and Failure Model Parameters Estimation of AISI-1045 Medium Carbon Steel for Metal Forming Applications, Materials 12 (4).

Özel, Tuğrul, and Yiğit Karpat. (2007). Identification of Constitutive Material Model Parameters for High-Strain Rate Metal Cutting Conditions Using Evolutionary Computational Algorithms, Materials and Manufacturing Processes 22 (5): 659–67.

Piegl, L. (1988). Curve and Surface Fitting: An Introduction. Computer-Aided Design. Vol. 20.

Poloni, Carlo, Andrea Giurgevich, Luka Onesti, and Valentino Pediroda. (2000), Hybridization of a Multi-Objective Genetic Algorithm, a Neural Network and a Classical Optimizer for a Complex Design Problem in Fluid Dynamics, Computer Methods in Applied Mechanics and Engineering 186 (2–4): 403–20.

Remache D, Semaan M, Rossi JM, Pithioux M and Milan JL (2019). Application of the Johnson-Cook Plasticity Model in the Finite Element Simulations of the Nanoindentation of the Cortical Bone, Journal of the Mechanical Behavior of Biomedical Materials.

S. Cooreman · D. Lecompte · H. Sol J. Vantomme · D. Debruyne (2008). Identification of Mechanical Material Behavior Through Inverse Modeling and DIC, Experimental Mechanics.

Saha, Sriparna, and Sanghamitra Bandyopadhyay (2013). A Generalized Automatic Clustering Algorithm in a Multiobjective Framework, Applied Soft Computing Journal 13 (1): 89–108.

Shrot, Aviral, and Martin Bäker (2012). Determination of Johnson-Cook Parameters from Machining Simulations, Computational Materials Science 52 (1): 298–304.

Stefan Hartmann, Rose Rogin Gilbert. (2021). Material Parameter Identification Using Finite Elements with Time-Adaptive Higher-Order Time Integration and Experimental Full-Field Strain Information, Computational Mechanics.

Stenberg, N., C. Fellers, and S. Östlund. (2001). Plasticity in the Thickness Direction of Paperboard under Combined Shear and Normal Loading, Journal of Engineering Materials and Technology, Transactions of the ASME 123 (2): 184–90.

Stenberg, Niclas. (2003). A Model for the Through-Thickness Elastic-Plastic Behaviour of Paper, International Journal of Solids and Structures 40 (26): 7483–98.

Tien, Dao Lien, Nguyen Thi Thu Phuong, Duong Pham Tuong Minh, and Viet Dung Luong. (2023). Finite Element Simulation for the Plastic Behavior of Corrugated Core Sandwich Panel, Journal of the Serbian Society for Computational Mechanics 17 (2): 142–52.

Titu, Nesar Ahmed, Matt Baucum, Timothy No, Mitchell Trotsky, Jaydeep Karandikar, Tony L. Schmitz, and Anahita Khojandi (2021). Estimating Johnson-Cook Material Parameters Using Neural Networks, In Procedia Manufacturing, 53:680–89.

Wang, Xin, Tao Jiang, Chong Ji, Changxiao Zhao, Yuting Wang, and Zhenru Gao, (2023). Mechanical Properties and Constitutive Modeling of 6063-T5 Aluminum Alloy Over a Wide Range of Strain Rates and Temperatures, International Journal of Thermophysics 44 (9).

Wangtian Yin, Yongbao Liu, Xing He and Zegang Tian. (2024). Parametric Analysis and Improvement of the Johnson-Cook Model for a TC4 Titanium Alloy, Metals.

Zhang, Honglei, Xuehui Lin, Yanqun Wang, Qian Zhang, and Yilan Kang. (2010). Identification of Elastic-Plastic Mechanical Properties for Bimetallic Sheets by Hybrid-Inverse Approach, Acta Mechanica Solida Sinica 23 (1): 29–35.